Improved indicators of cell membrane potential that use fluorescence resonance energy transfer

Jesús E González* and Roger Y Tsien

Background: Fluorescence detection of cell membrane potentials is an important technique in neurobiology, cell physiology and pharmaceutical screening, but traditional one-fluorophore indicators either respond too slowly or have limited sensitivity. Recently, we introduced two-component sensors based on the transfer of fluorescence resonance energy from fluorescent lectins bound on one side of the plasma membrane to highly fluorescent oxonol acceptors that electrophorese from one face of the membrane to the other in response to membrane potential.

Results: We have found that fluorescent lectins can often be advantageously replaced in such sensors by fluorescently labeled phospholipids. A coumarin-labeled phosphatidylethanolamine donor and a bis(1,3-dihexyl-2-thiobarbiturate)trimethineoxonol acceptor gave the largest sensitivity of fluorescence ratio (>50% per 100 mV) ever reported. The response was also speeded several-fold by lengthening the mobile dye to the pentamethineoxonol analog, the <0.4 ms time constant of which was shorter than action potential durations. Photodynamic damage due to singlet oxygen was reduced by administering a natural carotenoid, astaxanthin.

Conclusions: Voltage-sensitive fluorescence resonance energy transfer already gives record-setting performance on single cells and will continue to be rationally improvable.

Address: Howard Hughes Medical Institute and Department of Pharmacology, 310 Cellular and Molecular Medicine West, University of California, 9500 Gilman Drive, La Jolla, CA 92093-0647, USA.

*Present address: Aurora Biosciences Corporation, 11149 North Torrey Pines Road, La Jolla, CA 92037, USA.

Correspondence: Roger Y Tsien
E-mail: rtsien@ucsd.edu

Key words: hydrophobic ions, membranes, oxonols, phospholipids, potentiometric fluorescent probes

Received: **27 January 1997**
Revisions requested: **21 February 1997**
Revisions received: **4 March 1997**
Accepted: **6 March 1997**

Chemistry & Biology April 1997, 4:269–277
http://biomednet.com/elecref/1074552100400269

Introduction

Membrane potentials provide the basis for bioenergetics in all cells and for fast or long-distance signal propagation in excitable tissues such as nerve and muscle. Optical detection of membrane potentials enables the measurement of electrical signals that is not possible with conventional microelectrodes [1–5]. Fluorescent probes can report membrane potentials in locations within a single cell that are inaccessible to electrodes, such as the fine processes of neurons. On a larger scale, imaging techniques enable the potentials of large assemblies of cells to be recorded simultaneously with high temporal and spatial resolution. Electrodes have also been used to monitor several neurons simultaneously in brain tissue, but the bulk and mechanical invasiveness of electrodes limits the number of cells that can be directly monitored with such techniques. Positron-emission tomography and functional magnetic resonance imaging are sufficiently noninvasive to be used on human brains, but they can only detect massed neuronal activity in coarse regions, typically millimeters across, with a time resolution of seconds or minutes. Voltage-sensitive indicators are important tools in high-throughput pharmaceutical screening for drugs that affect ion channels and transporters. Membrane potentials reflect the composite activity of such ion transport mechanisms, for which fluorescent indicators offer one of the few general assays that can be miniaturized and automated.

Advances in fluorescence detection and in the imaging of cellular electrical activity are dependent on improved voltage-sensitive fluorescence probes. Traditional dyes that respond quickly enough to record the electrical signaling of neurons are polymethines such as *p*-dialkylaminostyryl pyridinium compounds [4,6,7]. The best of these typically give 2–10% changes in fluorescence levels per 100 mV in a variety of biological samples [8]. The largest reported signal is a 21% per 100 mV change that was observed in a neuroblastoma cell [9]. These responses are much smaller than the 2–100-fold changes typical for fluorescent indicators of chemical analytes. Although much has been learned from existing indicators of membrane potential, many experiments are hindered by limited sensitivity. An even more fundamental problem is that many competing mechanisms exist for such small optical responses to membrane potential and it is therefore difficult to predict which mechanism will be operative for a given indicator in a given tissue. For this reason, much trial and error has been necessary to find dyes that are effective for each different biological preparation [10].

Recently, we introduced a rational mechanism [11] and the molecules necessary for fast ratiometric voltage-sensitive fluorescence resonance energy transfer (FRET) in single cells (Fig. 1). The voltage sensor is a hydrophobic

Figure 1

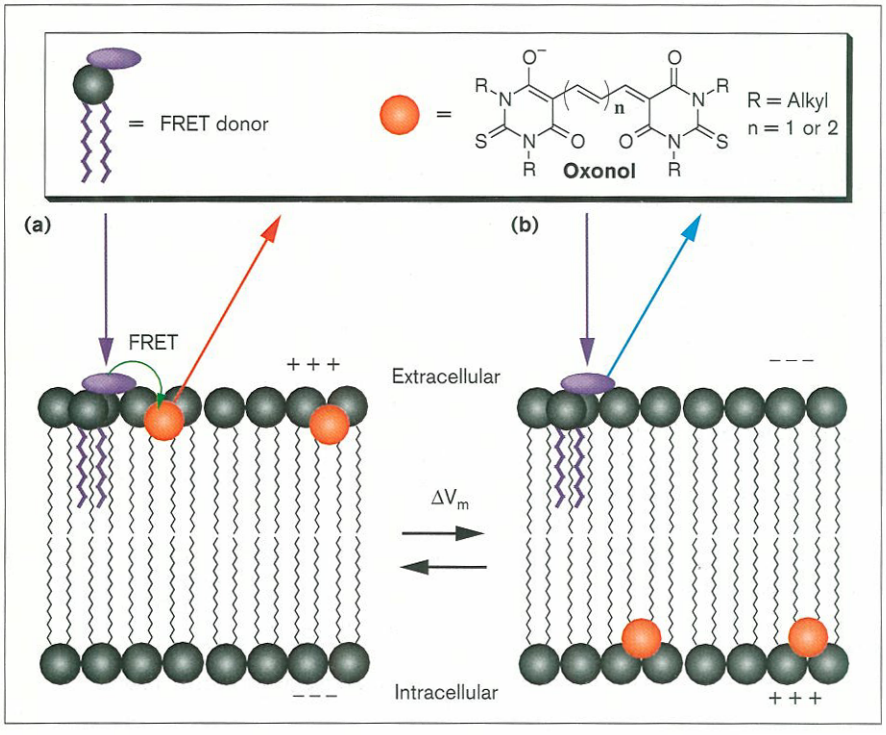

A scheme illustrating the FRET mechanism. In this case, the impermeant fluorophore is located on the extracellular face of the plasma membrane and functions as the donor, while the oxonol functions as the acceptor. **(a)** At normal negative resting membrane potentials, the oxonol molecules bind predominantly to the extracellular membrane surface and allow significant FRET. **(b)** Upon depolarization (ΔV_m), the oxonol molecules translocate to the intracellular binding site and FRET is diminished, resulting in an enhancement of the donor emission and a decrease in the acceptor emission. The generic oxonol structure is shown.

fluorescent anion that binds tightly to the plasma membrane at two energy minima at the intracellular and extracellular membrane–water interfaces. The ratio of the fluorophore concentrations at the two interfaces is an exponential function of the transmembrane potential, as described by the Nernst equation. When the membrane potential changes, the hydrophobic anions rapidly redistribute between the two sides of the plasma membrane to establish a new equilibrium that is appropriate for the new transmembrane potential. We showed that bis-(1,3-dihexyl-2-thiobarbiturate)-trimethineoxonol, $DiSBAC_6(3)$, redistributes between the intracellular and extracellular membrane sites in 2–3 ms. A ratiometric fluorescent readout is created by labeling just one side (typically the extracellular face) of the plasma membrane with a second fluorophore that can undergo FRET with the mobile oxonol voltage sensor. At negative membrane potentials — the norm for resting cells — the majority of the oxonol molecules are at the extracellular membrane binding site. Assuming that the acceptor is loaded at sufficient surface density, substantial FRET between the impermeant and mobile fluorophores occurs. When excitation is at wavelengths that match the donor absorbance, FRET causes the donor emission to be quenched and the acceptor emission to be enhanced. Upon plasma membrane depolarization, the oxonol molecules move to the intracellular binding site and FRET is decreased because the average distance between the immobile fluorophores and the mobile oxonol molecules has been increased. The decreased FRET causes the donor's emission to increase and the acceptor's emission to decrease. Because FRET works within the nanosecond lifetime of the donor, the overall kinetics are governed by the millisecond time scale for translocation of the fluorescent ion across the membrane. An additional advantage of this mechanism is its ratiometric output. The amplitudes at the donor and acceptor emission wavelengths respond in opposite directions, and their ratio gives a larger and more reliable signal than either emission alone. By using this ratio, several sources of experimental error are corrected including cell motion artifacts, fluctuations in cell number, excitation intensity, donor loading levels, and photobleaching of the donor.

Previously, we reported [11] that fluorescently labeled lectins, particularly wheat germ agglutinin (WGA), could function as FRET donors and acceptors with membrane-bound bis-(1,3-dialkyl-2-thiobarbiturate)-trimethineoxonols. The largest voltage-dependent signals in cells were achieved using fluorescein-labeled WGA (FL-WGA) as a donor to $DiSBAC_6(3)$. In astrocytoma cells, this pair, which we call FLOX6, gave ratio changes up to 34% for a 100 mV depolarization. Despite generating voltage-sensitive signals comparable to the best 'fast' dyes in single cells, the FLOXn pairs — combination of FL-WGA and $DiSBAC_n(3)$ — were far from ideal. First, FRET in the FLOXn systems did not optimally transduce the inherent voltage sensitivity of the oxonol into a usable ratiometric fluorescence change. The ratio of $DiSBAC_6(3)$

Figure 2

Reaction schemes. **(a)** Preparation of CC1-DMPE; (i) $CHCl_3$/dioxane, diisopropylethylamine (DIEA), N,N'-disuccinimidyl carbonate, (ii) $CHCl_3$/MeOH, DIEA, DMPE. **(b)** Synthesis of bis-(1,3-dialkyl-2-thiobarbiturate)-pentamethineoxonols $DiSBAC_n(5)$; (iii) pyridine.

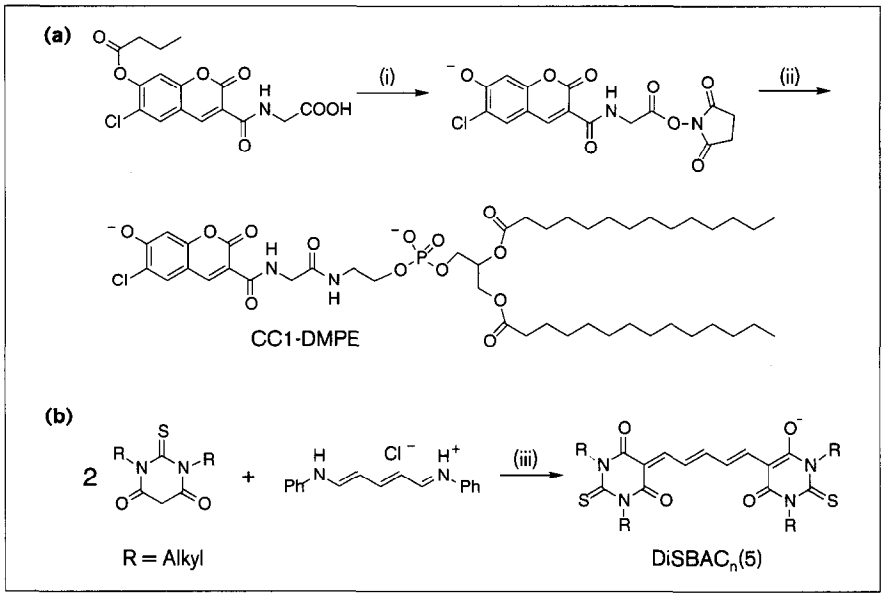

concentration at the intracellular and extracellular membrane binding sites, based on the voltage dependence of the displacement currents, changed about seven times more than the ratio of donor to acceptor emissions [11]. Second, the 2–3 ms translocation time constant for $DiSBAC_6(3)$ was too slow for action potentials with millisecond durations. Finally, it was difficult to load two dyes, including the very hydrophobic oxonol, at the correct stoichiometry into a thick complex tissue such as a brain slice. Below, we report molecular modifications that ameliorate the first two important shortcomings. We also show that exogenous carotenoids can be incorporated into the plasma membrane to reduce photodynamic damage due to singlet oxygen, the highly reactive and toxic form of O_2 in which all electrons are paired.

Results and discussion

Improved and extended voltage-sensitive FRET with trimethineoxonols

To improve the ability of FRET to signal the transbilayer distribution of permeant oxonol, we reasoned that it was important to maximize FRET between the donor and acceptor fluorophores on the same side of the membrane. Using a phospholipid instead of a lectin anchor, the immobile partner fluorophore could be put at the membrane–water interface instead of on the end of a cell-surface carbohydrate, thus substantially decreasing the distance of closest approach between the donor and acceptor. In addition, phospholipid loading should be more uniform from cell type to cell type because it is no longer dependent on the abundance of *N*-acetylglucosamine groups. Because R_0, the Förster distance at which FRET is 50% efficient, is 50 Å for the FLOX pairs and thus exceeds the distance across the membrane, some energy transfer occurs between donors and acceptors on opposite sides as well as on the same side of the membrane. Pagano and coworkers [12] have demonstrated such transbilayer FRET between fluorescent phospholipids in vesicle bilayers. Consequently, a smaller R_0 is also desirable and should result in increased FRET discrimination between the mobile ions on the extracellular faces compared with the intracellular faces of the membrane, because the distance the oxonol moves across the bilayer becomes larger relative to R_0. A simple way to decrease R_0 while maintaining bright fluorescence from both donor and acceptor is to increase the wavelength separation between the donor emission and the acceptor excitation spectra. On the basis of these considerations, we have developed a new FRET donor to voltage-sensitive oxonol molecules that gave the largest ratio signal observed in a cell to date.

A coumarin-labeled phospholipid — N-(6-chloro-7-hydroxy-2-oxo-2H-1-benzopyran-3-carboxamidoacetyl)-dimyristoylphosphatidylethanolamine (CC1-DMPE) — was prepared and found to be an excellent voltage-sensitive FRET donor to bis-(1,3-dialkyl-2-thiobarbiturate)-trimethineoxonols. The fluorescent phospholipid was prepared by coupling the N-hydroxy-succinimidyl ester of 7-butyryloxy-6-chloro-2-oxo-2H-1-benzopyran-3-carboxamidoacetic acid with *sn*-1,2-dimyristoylphosphatidylethanolamine (DMPE), as shown in Figure 2a. The 3-carbonyl and 6-chloro substituents lower the coumarin pK_a to well below physiological pH. Despite the compactness of its chromophore, comparable to anthracene, CC1-DMPE has an absorbance maximum of 414 nm and an extinction coefficient of ~40 000 $M^{-1}cm^{-1}$ in 2:1 methanol:Hanks balanced

Figure 3

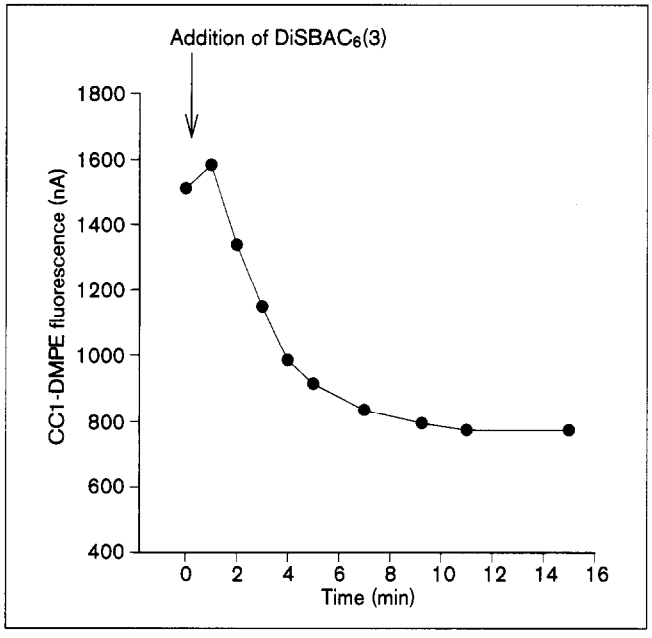

Quenching of CC1-DMPE-stained LM-(TK⁻) cells upon addition of 2.33 μM $DiSBAC_6(3)$. The CC1-DMPE emission, measured as nA of photomultiplier current, is quenched ~50% in ~15 min.

Figure 4

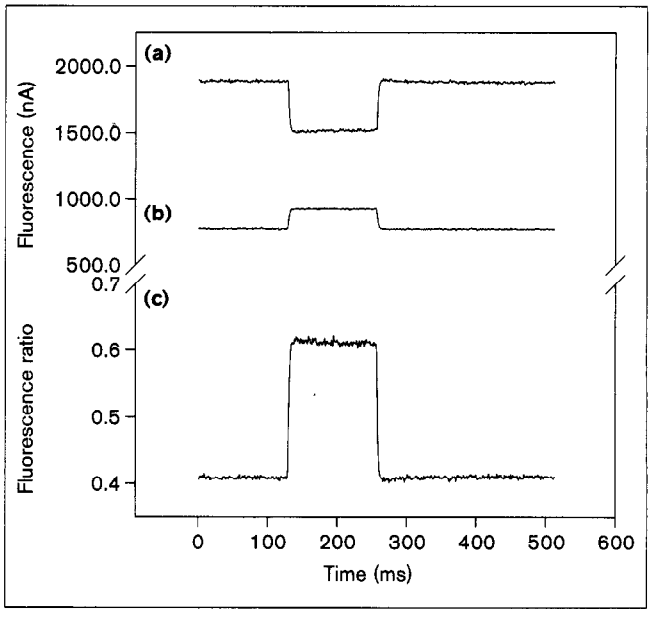

Voltage-sensitive FRET changes in a voltage-clamped LM-(TK⁻) cell stained with C063 and subjected to a 100 mV depolarization step. The emissions of **(a)** $DiSBAC_6(3)$ and **(b)** CC1-DMPE, and **(c)** the ratio of the latter to the former are shown. The 100 mV depolarization increases the ratio by 50%. The traces are the average of 16 sweeps.

salt solution (HBSS). Its fluorescence quantum yield is indistinguishable from 1.0 within experimental error. The calculated R_0 for the CC1-DMPE/$DiSBAC_6(3)$ pair is 46 Å. For brevity, this pair of molecules is called CO63, where C stands for coumarin, O for oxonol, 6 for the alkyl chain length on the oxonol, and 3 for the number of polymethine carbons; the numbers in the FRET pair name therefore refer to number of methines and alkyl carbons on the oxonol.

Mammalian cells were loaded by diluting a DMSO stock solution of CC1-DMPE with HBSS and adding it to the bath solution. Stained cells excited at 405 nm showed blue fluorescence localized to the plasma membrane. FRET in single cells could be directly observed by the addition of trimethineoxonol to CC1-DMPE-stained cells. As shown in Figure 3, loading $DiSBAC_6(3)$ into the plasma membrane of LM-(TK⁻) cells resulted in FRET and caused the CC1-DMPE fluorescence to be quenched by 50%. This new FRET pair gave up to an 80% ratio change for a 100 mV depolarization in an astrocytoma cell, the largest millisecond voltage-sensitive optical signal observed in a cell to date. Normally, ratio changes of 40–60% are observed for 100 mV depolarization, with a greater change occurring in the CC1-DMPE signal (Fig. 4). The voltage sensitivity of the COn3 pair was consistently two to three times better than that of the FLOXn pairs in a variety of cell types. In addition, the increased spectral separation facilitated discrimination of the donor and acceptor emissions and reduced direct excitation of the acceptor. The fluorescence emission due to direct excitation of $DiSBAC_6(3)$ at 405±15 nm was negligible at 3–10%, usually <5% of the total oxonol emission.

In neonatal cardiomyocytes, 5–30% fluorescence ratio changes were observed for spontaneously generated action potentials. The largest signals were almost four times larger than those recorded with the FLOXn pairs. An example of such a large change from a cluster of heart cells is given in Figure 5, which also demonstrates the benefits of ratio output. The individual wavelengths, shown at the top of the figure, show a slowly decreasing baseline at both wavelengths that is due to fluorophore bleaching. The ratio data shown on the bottom of the figure compensate for the loss of intensity in both channels and result in a flat baseline.

Voltage-sensitive FRET is highly dependent on the membrane surface densities of the donor and acceptor molecules. The most important criterion for attaining the largest voltage-sensitive fluorescence changes is to attain acceptor membrane concentrations sufficient to quench most of the emission from the donors on the same side of the membrane. Astrocytoma and LM-(TK⁻) cells typically give a whole-cell capacitance of 15 pF before loading; this corresponds to a plasma membrane surface area of 1.5×10^{-5} cm^2 assuming the usual specific capacitance of 1 μF cm^{-2} for

Figure 5

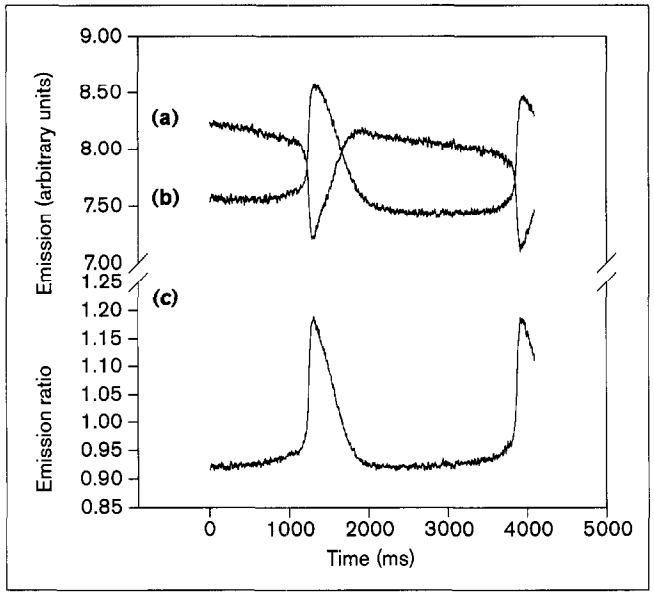

A 30% fluorescence ratio change in a spontaneously beating cluster of neonatal cardiomyocytes stained with CO63. The emissions of **(a)** $DiSBAC_6(3)$ and **(b)** CC1-DMPE and the ratio **(c) = (b)/(a)** are shown.

biological membranes. Cells that are heavily loaded with $DiSBAC_6(3)$ have about 9.5 pC of oxonol per cell [11], and therefore a density of one oxonol per 2500 Å^2 of bilayer. At typical negative resting membrane potentials, most of the oxonol molecules should be on the extracellular leaflet of the plasma membrane, at about one oxonol per 50 Å square. Because for COn3 pairs $R_0 = 46$ Å, it is not surprising that the above surface concentrations of acceptor are needed for maximally efficient intermolecular quenching of the donor. Provided such concentrations can be attained by suitable adjustment of dye loading concentration and time, the ratio responses typically vary by no more than a factor of two between different tissue culture cell lines.

In theory, it would be preferable for the mobile ion to serve as a FRET donor rather than as an acceptor, because efficient FRET does not require the donor to be at a high surface concentration. Lowering the surface density of the mobile ions would minimize the electrostatic repulsion between them as well as the capacitative load on the cell [11]. Improvements have been made in this area. $DiSBAC_6(3)$ was successfully used as a FRET donor to Cy5-labeled DMPE (Cy5-DMPE) in B104 neuroblastoma cells. The ratio changes of 5–15% per 100 mV are the largest that have been observed with the mobile ion as the donor. Previously, with Texas Red WGA as the acceptor, only 1–2% changes were recorded [11]. The larger signal found with this molecular configuration is most likely to be due to the higher membrane concentration possible with a phospholipid acceptor rather than a lectin.

Longer wavelength and faster voltage-sensitive FRET with pentamethineoxonols

The main kinetic barrier to translocating a hydrophobic ion across the membrane is the electrostatic energy necessary to move the charge of the ion away from an aqueous medium of high conductivity and dielectric constant towards the hydrocarbon-like center of the membrane. Increasing the hydrophobicity of the ion decreases the energy barrier and increases the speed of translocation because the ion is initially buried deeper in the membrane, so the energy well at the interface is not as deep [13,14]. Thus, increasing the length of the four alkyl chains on the oxonol from C_2 to C_4, C_6, and C_{10} decreases the time constant from hundreds of milliseconds to ~2 ms. But such simple chain extension outside the chromophore reaches a point of diminishing returns in faster translocation speeds and it introduces a severe problem in getting enough dye dissolved in the aqueous medium for it to stain cells. To achieve yet faster speeds, we decided to increase the charge delocalization by adding two methine units to the polymethine chain. The extra vinyl increases the length of the chromophore by about 33% and correspondingly decreases the Born charging energy, which is inversely proportional to the ionic radius. Charge delocalization is critical for lowering the activation barrier for ion translocation across the core of the membrane [15], which has a low dielectric constant.

The bis-(1,3-dialkyl-2-thiobarbiturate)-pentamethineoxonols were prepared by condensing 1,3-substituted thiobarbituric acids with N-[5-(phenylamino)-2,4-pentadienylidene]aniline hydrochloride (Fig. 2b). The pentamethineoxonol molecules absorb at 638 nm with an extinction coefficient of 225 000 $M^{-1}cm^{-1}$, and they emit maximally at 663 nm in ethanol. The absorbance and emission are shifted 100 nm to longer wavelengths than those of the trimethineoxonol — the typical effect of lengthening a symmetrical polymethine chromophore by one vinyl group [16]. The longer wavelength means that the oxonol can be an acceptor from a larger number of donors, thus giving more experimental flexibility for excitation and emission wavelengths. In addition, the longer wavelengths show less overlap with cellular autofluorescence and penetrate tissue better due to reduced scattering and absorbance by endogenous pigments such as heme groups. The pentamethines can be loaded into cells in culture in the same manner as the trimethineoxonols. Bis-(1,3-dibutyl-2-thiobarbiturate)-pentamethineoxonol, $DiSBAC_4(5)$, can be loaded in HBSS bath solution, while the hexyl compound, $DiSBAC_6(5)$, requires addition of β-cyclodextrin in order to mask the hexyl sidechains and solubilize the hydrophobic oxonol in the aqueous bath solution. Voltage-sensitive FRET from various plasma-membrane-bound fluorescent donors to the pentamethineoxonols has been achieved in single cells. FL-WGA transferred excited state energy to the pentamethineoxonol and gave ratio changes comparable to those observed for

Figure 6

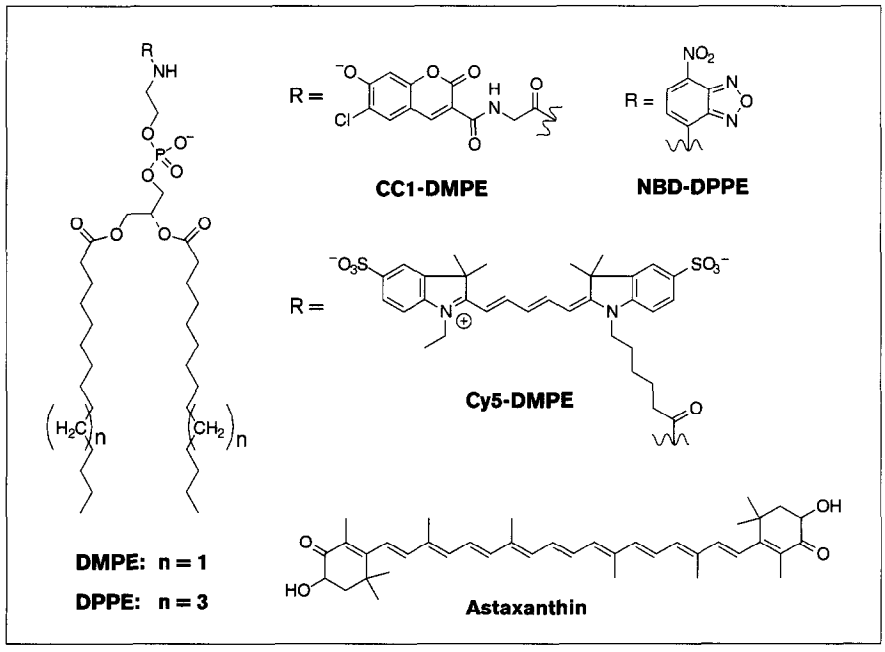

Structures of the relevant fluorescently labeled membrane-impermeant phosphatidylethanolamine conjugates and the photoprotective carotenoid astaxanthin.

the trimethineoxonol. In astrocytoma cells, ratio changes of 15–30% were recorded for a 100 mV depolarization step from –70 mV. The decrease in FRET due to the reduced overlap integral on moving the oxonol absorbance 100 nm to longer wavelengths is compensated by increased FRET selectivity between the two membrane oxonol binding sites and decreased spectral overlap.

Fluorescent phosphatidylethanolamine (PE) conjugates can also function as FRET donors to the pentamethineoxonols. The structures of the PE conjugates we tested are shown in Figure 6. The N-(7-nitrobenz-2-oxa-1,3-diazol-4-yl)-dipalmitoylphosphatidylethanolamine conjugate, NBD-DPPE, functioned as a FRET donor to the pentamethineoxonols and gave 1–10% ratio changes per 100 mV. The CC1-DMPE/DiSBAC$_6$(5) pair (CO65) gave 15–30% ratio changes in voltage-clamped astrocytomas for 100 mV depolarization. CO65 is remarkable because the CC1-DMPE emission and DiSBAC$_6$(5) absorbance maxima are separated by 213 nm and the overlap of the normalized spectra looks very small (Fig. 7). The unity quantum yield of the CC1-DMPE donor and the huge extinction of the pentamethineoxonol acceptor nevertheless gave a calculated R_0 of 37 Å. This FRET pair essentially spans the entire visible range.

Importantly, the membrane translocation rates for the pentamethines were five to nine times faster than the trimethine analogs, as we hoped. Displacement currents of DiSBAC$_4$(5) in voltage-clamped astrocytoma cells showed that the oxonol jumps across the plasma membrane with a time constant of ~2 ms in response to voltage steps of 20–120 mV. The time constant for the trimethine analog is ~18 ms under identical conditions. The displacement currents of DiSBAC$_6$(5) were too fast to allow them to be

Figure 7

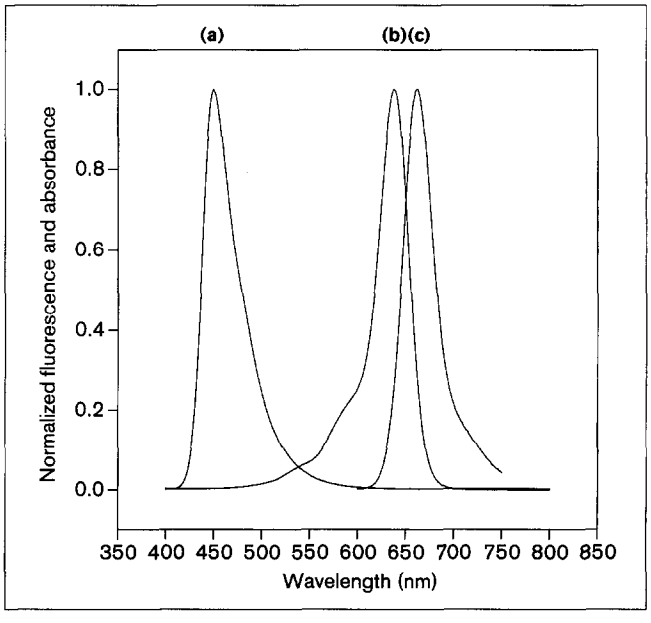

Spectra of the CC1-DMPE/DiSBAC$_6$(5) (CO65) FRET pair. **(a)** The fluorescence emission spectrum of CC1-DMPE in 2:1 methanol:HBSS. **(b)** The absorbance spectrum and **(c)** the emission spectrum of DiSBAC$_6$(5) in ethanol. These spectra were used to calculate R_0=37 Å.

resolved easily from the capacitance-charging currents, but the FRET from CC1-DMPE to $DiSBAC_6(5)$ had a $383 \pm 32\,\mu s$ time constant in response to a depolarization step from 0–100 mV. The ratio data and the exponential response are shown in Figure 8. The translocation of $DiSBAC_6(5)$ in cells was about six times faster than that of the trimethine analog $DiSBAC_6(3)$ and second only to 2,4,6,2′,4′,6′-hexanitrodiphenylamine, which was nonfluorescent. Judging by the temperature coefficient for translocation of related oxonol molecules [11], the time constant should be around 100 μs at 37°C. The submillisecond response would allow reliable registration of the action potentials of single neurons and should be sufficient for all but the small minority of experiments that require the fastest time resolution.

Figure 8

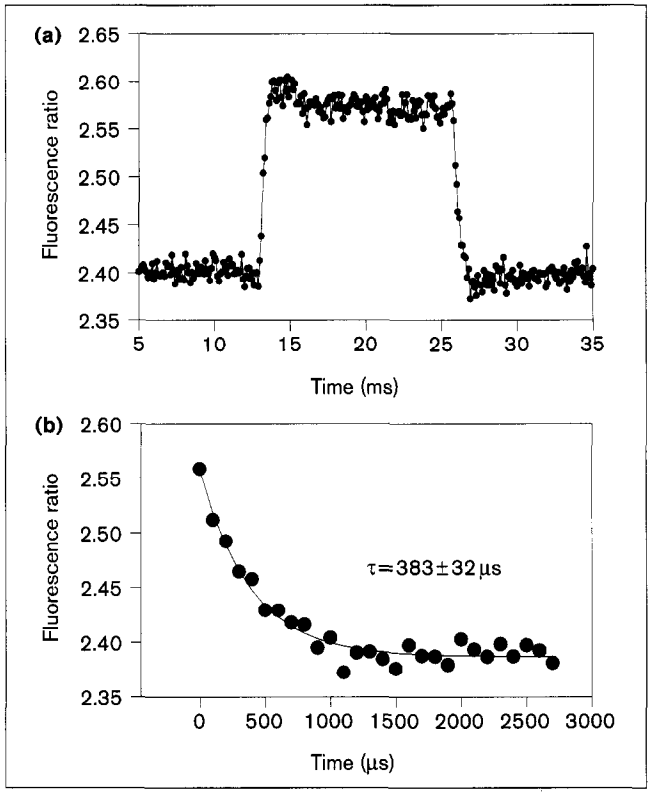

$DiSBAC_6(5)$ translocates with a time constant of 383 ± 23 μs in response to a 100 mV positive voltage step from −70 mV and causes a rapid FRET ratio change in LM-(TK^-) cells stained with CO65. **(a)** The complete fluorescence ratio response to the voltage step. **(b)** The response to the return to −70 mV, displayed with expanded time resolution. The trace is the average of 64 sweeps acquired at 10 kHz.

Exogenous carotenoids protect cells from photodynamic damage

Biological applications of voltage-sensitive dyes are often limited by photodynamic damage. Because the signal changes are small, strong illumination is necessary to attain usable signal-to-noise ratios. Compounding the problem is the localization of the dyes in the plasma membrane, which contains both O_2 and a variety of vital lipid and protein components that are susceptible to oxidative damage. Photosynthetic membranes, despite having very high quantum yields, still make use of carotenoids to scavenge harmful sensitized products such as singlet oxygen [17].

Previous attempts to reduce photodynamic damage by administrating extremely hydrophobic carotenoids such as β-carotene were unsuccessful, perhaps because not enough carotene reached the membrane (B.M. Salzberg, A.L. Obaid and T.D. Parsons, personal communication). We chose astaxanthin for two reasons: in model membranes it is the best carotenoid for quenching reactive oxygen species [18–21], and it contains α-hydroxy ketone groups on each end of the molecule (Fig. 6), which should give it more water solubility than other carotenoids. In addition, astaxanthin is responsible for the pink color in salmon and lobster [22] and is therefore unlikely to be toxic.

Spontaneously beating neonatal cardiomyocytes stained with FLOX6 are a good system in which to assess photodynamic damage because they are quite sensitive to 488 nm laser light and abruptly stop beating and freeze in a contracted state. Similar severe photodynamic damage in isolated cardiomyocytes has been reported with other voltage-sensitive dyes [23]. The phototoxic effect was absent in cells stained only with FL-WGA and was observed in cells stained only with $DiSBAC_6(3)$. Clearly, under these conditions, the membrane-bound oxonol had a phototoxic effect, probably via the production of singlet oxygen.

To test whether exogenous astaxanthin could reach cell membranes, Jurkat lymphocytes were loaded by the protocol of Cooney *et al.* [24], which uses the ability of tetrahydrofuran (THF) to disperse the carotenoid in aqueous media. The cells gave a reddish pellet upon centrifugation. The color of the astaxanthin could not be washed away and the stained cells showed a broad absorbance from 400–540 nm similar to that seen for the carotenoid in organic solvents. The same loading protocol was therefore applied to cardiomyocytes prior to FLOX staining. For equal illumination intensities at 488 nm delivered by a laser scanning confocal microscope [25], cells loaded with astaxanthin could be irradiated ten times longer before they stopped beating, 58 ± 9 s compared with 5.4 ± 0.5 s for unprotected controls. The protective effect was not due to trivial absorption of the excitation light because both the absolute fluorescence and the voltage-dependent optical signals from the FLOX dyes were comparable to those of cells not loaded with astaxanthin. To our knowledge, this is the first example in which photodynamic damage due to voltage-sensitive dyes has been inhibited by exogenous quenchers of singlet oxygen.

Significance

Membrane potentials are central to energy generation and excitable signal transmission in cells. They can be optically monitored by fluorescence resonance energy transfer between a mobile lipophilic ion and a partner fluorophore anchored on the extracellular side of the membrane. The amplitude of the fluorescence changes may be optimized by tethering the stationary fluorophores to the phospholipid head groups and adjusting the spectral overlap to reduce transbilayer energy transfer and direct excitation of the acceptor. The speed of response is improved by increasing the delocalization of negative charge within the mobile ion. Photodynamic damage may be reduced by incorporating quenchers of singlet oxygen into the membrane. The remaining challenges are to combine all these improvements into a single set of molecules and to devise reliable means of delivering them with the appropriate stoichiometry to specific cells within relatively intact tissues.

Materials and methods

All starting materials and reagents were of the highest purity available (Aldrich, Milwaukee, WI, USA) and used without further purification, except where noted. L-α-DMPE and NBD-DPPE were purchased from Sigma (St Louis, Missouri, USA). Solvents were HPLC grade (Fisher) and were dried over activated molecular sieves, 3 Å. Nuclear magnetic resonance (NMR) spectra were acquired on a Varian Gemini 200 MHz spectrometer (Palo Alto, CA, USA). The spectra were referenced relative to the residual solvent peak ($CHCl_3$, δ = 7.24 ppm; d_6-DMSO, δ = 2.50 ppm; CD_3OD, δ = 3.31 ppm). Fluorescence spectra were taken on a SPEX Fluorolog-2 (Edison, NJ, USA) and were corrected for lamp and detector wavelength variations using the manufacturer supplied correction files.

6-Chloro-7-hydroxy-2-oxo-2H-1-benzopyran-3-carboxamido-acetic acid-N-hydroxysuccinimide ester (CC1-NHS)

7-Butyryloxy-6-chloro-2-oxo-2H-1-benzopyran-3-carboxamidoacetic acid (a generous gift of Gregor Zlokarnik; 52 mg, 100 μmol) was dissolved in 0.75 ml of 1:2 $CHCl_3$/dioxane. Diisopropylethylamine, DIEA, (42 μl, 31 mg, 238 μmol) was added to the solution. The solution was gently heated to try to dissolve some of the insoluble solids. After cooling back to room temperature, 80 mg of N,N′-disuccinimidylcarbonate, technical grade, (~ 281 μmol) was added to the reaction mixture. After 4 h, the reaction was mixed with about 30 ml of ethyl acetate and washed 3× with water. The organic layer was dried over anhydrous $NaSO_4$ and the solvent was removed under vacuum, yielding 43 mg of solid. The solid was then triturated with $CHCl_3$ and centrifuged, yielding 15 mg of product (27%) which gave a single spot by thin layer chromatography, TLC. ^{1}H NMR (d_6-DMSO): δ 9.17 (t, J = 5.9 Hz, 1H, amide), 8.86 (s, 1H, coumarin), 8.13 (s, 1H, coumarin), 6.99 (s, 1H, coumarin), 4.52 (d, J = 6.0 Hz, 2H, glycine), 2.83 (s, 4H, succinimidyl). Electrospray (negative ion) mass spectrometry [MeOH : H_2O; 95:5] (peak, rel. int.) 278.0 (50), 310.0 (25), 393.2 (M-1, 100), 395.0 (M-1, 25); calc'd M = 393.2 Da and 395.2 Da for the ^{35}Cl and ^{37}Cl isotopes, respectively.

N-(6-Chloro-7-hydroxy-2-oxo-2H-1-benzopyran-3-carboxamido-acetyl)-dimyristoylphosphatidylethanolamine (CC1-DMPE)

10 mg of L-α-DMPE (15.7 μmol) was dissolved in 1 ml of 2:1 dry $CHCl_3$: CH_3OH. DIEA (3.3 μl, 18.8 μmol) was added to the reaction solution. 9.3 mg of CC1-NHS was added with stirring, some of which did not dissolve immediately. After 3.5 h all the solid had dissolved and TLC indicated that the reaction was complete. The reaction flask was left stirring overnight. The solvents were removed under vacuum and the residue was dissolved in 1–2 ml of 2:1 MeOH : H_2O. The reaction mixture was applied to a C_{18} reverse phase (BAKERBOND) column (1.7 × 7 cm). Polar impurities were removed eluting with the same solvent system. The desired product was eluted off the column with 9:1 MeOH : H_2O. Fractions containing only the desired product were pooled and concentrated on a rotary evaporator. The water caused the solution to bump very badly. After drying under high vacuum, 14.1 mg of product was attained (90% yield). The product eluted as a single fluorescent spot on reverse phase TLC. ^{1}H NMR (CD_3OD): δ 9.37 (br t, J = 5.2 Hz, ~1H, amide), 8.75 (s, 1H, coumarin), 8.28 (br t, J = 5.6 Hz, ~1H, amide), 7.85 (s, 1H, coumarin), 6.90(s, 1H, coumarin), 5.24 (cm, 1H, *sn*-2-glycerol), 4.44 (dd, J_1 = 12.1 Hz, J_2 = 3.2 Hz, 1H, glycerol), 4.20 (dd J_1 = 12.0 Hz, J_2 = 6.8, 1H, glycerol), 4.13 (d, J = 6.6 Hz, 2H, glycine), 3.99 (t, J = 5.6 Hz, 2H, $RNCH_2CH_2OR'$), 3.91 (cm, 2H, glycerol), 3.47 (cm, 2H, $RNCH_2CH_2OR'$), 2.30 (cm 4H, CH_2 α to carbonyl), 1.59 (cm, 4H, CH_2 β to carbonyl), 1.2–1.4 (cm, 40H, bulk CH_2s, 0.90 (t, J = 6.5 Hz, 6H, CH_3). Electrospray (negative ion) mass spectrometry [MeOH : H_2O; 95:5] (peak, rel. int.) 456.8 (M-2, 20), 524.5 (50), 704.9 (6), 734.7 (100), 913.9 (M-1, 95); deconvoluted M = 915.3 Da; calc'd M = 915.5 Da. UV-vis (MeOH : HBSS; 2:1) λ_{max} = 414 nm. Fluorescence (MeOH : HBSS; 2:1) λ_{emax} = 450 nm, quantum yield = 1.0 determined using 9-aminoacridine in H_2O as a standard (quantum yield = 0.98) [26].

Cy5-DMPE

DMPE (1.0 mg, 1.6 μmol) was dissolved in 650 μg of (12:1) $CHCl_3$: MeOH, followed by addition of DIEA (1 ml, 5.7 μmol). Separately, Cy5.29.OSu monofunctional (a generous gift from Alan Waggoner) [27] (0.8 mg, 1 μmol) was dissolved in 150 μl of (2:1) $CHCl_3$: MeOH and added to the phospholipid solution. After 3 h, the solvent was removed under vacuum. The residue was dissolved in MeOH and loaded on a C_{18} reverse phase column (1 × 10 cm) equilibrated with 1:1 MeOH : H_2O. Eluting with the same solvent, the hydrolyzed ester was removed. The polarity was decreased to 9:1 MeOH : H_2O and the blue product was eluted off the column, yielding 400 μg (300 nmol, 30%). The amount of product was further confirmed by the measurement of the extinction coefficient. The measured value was within 20% of the expected value of 250 000 M^{-1} cm^{-1}.

Bis-(1,3-dihexyl-2-thiobarbiturate)-pentamethineoxonol [DiSBAC$_6$(5)]

1,3-Dihexyl-2-thiobarbituric acid (200 mg, 0.64 mmol) and N-[5-(phenylamino)-2,4-pentadienylidene]aniline hydrochloride (91 mg, 0.32 mmol) were mixed in 1 ml pyridine. The solution turned blue within 10 s. After letting the reaction mixture stir for 1.5 h, the solvent was removed under high vacuum. The residue was dissolved in $CHCl_3$ and chromatographed on silica gel eluting with a 93:7 $CHCl_3$: MeOH solution. The blue oxonol (72 mg, 31%) was recovered and was pure according to TLC. ^{1}H NMR ($CDCl_3/CD_3OD$): δ 7.60–7.80 (cm, 4H, methines), 7.35 (t, J = 11.3 Hz, 1H, central methine), 4.31 (cm, 8H, NCH_2R), 1.57 (cm, 8H, NCH_2CH_2R), 1.20 (br m, 24H, bulk methylenes), 0.74 (br t, 12H, methyl). Electrospray (negative ion) mass spectrometry [MeOH : H_2O; 95:5] (peak, rel. int.) 605.4 (M-1-80, 6), 669.4 (M-1-16, 4), 685.4 (M-1, 100); calc'd M = 686.0 Da. Fluorescence quantum yield was measured at 0.67 ± 0.1 in octanol using oxazine 1 in ethanol (quantum yield = 0.11) and 1,2-dichloroethane (quantum yield = 0.44) as standards [28].

Cells and staining

All cells were grown and handled as described for LM-(TK$^-$) except where noted. LM-(TK$^-$) cells were grown in Dulbecco's Modified Eagle Media, DMEM, (Gibco; Grand Island, NY, USA) with 10% fetal bovine serum (FBS) and 1% penicillin : streptomycin, PS, (Gemini; Calabasas, CA, USA). B104 cells were differentiated with 1 μM retinoic acid for five days prior to use. The cells were plated on 25 mm glass coverslips at least one day before use. The coverslips were mounted with silicone grease over circular holes in the bottom of plastic culture dishes. The adherent cells were washed and maintained in 2.25 ml of HBSS with 1 g l^{-1} glucose and 20 mM HEPES at pH 7.4.

Cells were sufficiently stained with 1–4 μM CC1-DMPE for 20 min. The appropriate concentration was achieved by diluting, with vortexing, a

2.3 mM DMSO stock solution with HBSS. β-Cyclodextrin, ~5 mg, was dissolved in 750 μl of the bath solution. The solution was then added with vortexing to 2 μl of a 2.33 mM oxonol DMSO stock solution and immediately added to the cells. The dye was left for 30–40 min at a bath concentration of ~2.3 μM. The excess dye was removed with 3–5 washes with HBSS. The dye staining could be accomplished in any order, but staining first with CC1-DMPE, washing, and then observing the quenching resulting from FRET upon adding oxonol afforded the most experimental control.

The cardiac myocytes [29] were a gift of Kenneth Chien, UCSD, USA. The Jurkat lymphocyte suspensions were grown in RPMI media with 5% heat inactivated FBS and 1% PS. 15–20 ml aliquots of the cellular suspension were washed three times before and after dye staining by centrifugation at 100 g for 4 min followed by additions of fresh HBSS.

The astaxanthin loading procedure followed the protocol developed by Cooney *et al.* [24] for other carotenoids. Astaxanthin (kind gift of Chuck Hawthorne and Jerry Sepinwall, Hoffmann-La Roche, Nutley, NJ, USA) was dissolved at 2 mM in deaerated THF. 100 μl of this solution was added to 20 ml of cold DMEM with vortexing. The previous extracellular medium was replaced by the astaxanthin containing medium at room temperature, and then the cells were placed in the 37°C incubator. Experiments were done about 24 h after addition of the carotenoid-containing media.

Optical recordings

The optical setup is described for the CO63 FRET pair. The fluorescently labeled cells were excited with light from a 75 W xenon lamp passed through a 405 ± 15 nm excitation interference filter. The light was reflected onto the sample using a DM430 dichroic (Nikon). The emitted light was collected with a 40× Nikon (1.3 numerical aperture) objective, passed through a 435 nm long pass filter and directed to a 520 DCXR dichroic (Chroma; Brattleboro, VT, USA). The reflected light from this second dichroic was passed through a 470 DF60 bandpass filter and made up the CC1-DMPE signal. The transmitted light was passed through a 573DF35 bandpass filter (Omega; Brattleboro, VT, USA) and comprised the trimethineoxonol signal. For experiments using the trimethineoxonol as a donor to Cy5-DMPE, a 550 nm dichroic was used for excitation and a 650 nm dichroic was used to split the emission. The long wavelength Cy5-DMPE fluorescence was passed through a 665 nm DF65 bandpass filter. Voltage dependent fluorescence changes in single cells were measured using a Nikon microscope attached to a Photoscan II photometer equipped with two red sensitive R3896 PMTs (Hamamatsu, Bridgewater, NJ, USA) for dual emission recordings. Simultaneous optical and electrical recordings were acquired at 1–10 kHz using a homemade Axobasic program that acquires data with the LSAMPLE command.

Electrophysiology

Patch clamp recordings were made using an Axopatch-1D amplifier equipped with a CV-4 headstage from Axon Instruments (Foster City, CA, USA). The pH 7.4 intracellular solution used contained 125 mM potassium gluconate, 1 mM $CaCl_2$, 2 mM $MgCl_2$, 11 mM EGTA, 4 mM ATP, 0.5 mM GTP and 10 mM HEPES.

Acknowledgements

We are grateful to Pilar Ruiz-Lozano for the generously supplying the neonatal myocyte cultures and Pierre Vincent for his kind help with the photoprotection experiments on the laser scanning confocal microscope.

References

1. Salzberg, B.M. (1983). Optical recording of electrical activity in neurons using molecular probes. In *Current Methods in Cellular Neurobiology.* (Barker J.L., ed.), pp. 139–187, Wiley, NY, USA.
2. Cohen, L.B. & Lesher, S. (1985). Optical monitoring of membrane potential: methods of multisite optical measurement. In *Optical Methods in Cell Physiology.* (De Weer P. & Salzberg B.M., eds), pp. 71–99, Wiley, NY, USA.
3. Grinvald, A., Frostig, R.D., Lieke, E. & Hildesheim, R. (1988). Optical imaging of neuronal activity. *Physiol. Rev.* **68**, 1285–1366.
4. Loew, L.M. (1988). How to choose a potentiometric membrane probe. In *Spectroscopic Membrane Probes.* (Loew L.M., ed.), pp. 139–151, CRC Press, Boca Raton, USA.
5. Loew, L.M. (1993). Potentiometric membrane dyes. In *Fluorescent and Luminescent Probes for Biological Activity.* (Mason WT., ed.), pp. 150–160, Academic Press, San Diego, USA.
6. Grinvald, A., Hildesheim, R., Farber, I.C. & Anglister, L. (1982). Improved fluorescent probes for measurement of rapid changes in membrane potential. *Biophys. J.* **39**, 301–308.
7. Loew, L.M. & Simpson, L.L. (1981). Charge-shift probes of membrane potential: a probable electrochromic mechanism for *p*-aminostyrylpyridinium probes on a hemispherical lipid bilayer. *Biophys. J.* **34**, 353–365.
8. Ebner, T.J. & Chen, G. (1995). Use of voltage-sensitive dyes and optical recordings in the central nervous system. *Prog. Neurobiol.* **46**, 463–506.
9. Grinvald, A., Fine, A., Farber, I.C. & Hildesheim, R. (1983). Fluorescence monitoring of electrical responses from small neurons and their processes. *Biophys. J.* **42**, 195–198.
10. Ross, W.N. & Reichardt, L.F. (1979). Species-specific effects on the optical signals of voltage-sensitive dyes. *J. Membrane Biol.* **48**, 343–356.
11. González, J.E. & Tsien, R.Y. (1995). Voltage-sensing by fluorescence resonance energy transfer in single cells. *Biophys. J.* **69**, 1272–1280.
12. Wolf, D.E., Winiski, A.P., Ting, A.E., Bocian, K.M. & Pagano, R.E. (1992). Determination of the transbilayer distribution of fluorescent lipid analogues by nonradiative fluorescence resonance energy transfer. *Biochemistry* **31**, 2865–2873.
13. Ketterer, B., Neumcke, B. & Läuger, P. (1971). Transport mechanism of hydrophobicions through lipid bilayer membranes. *J. Membrane Biol.* **5**, 225–245.
14. Andersen, O.S. & Fuchs, M. (1975). Potential energy barriers to ion transport within lipid bilayer. *Biophys. J.* **15**, 795–830.
15. Benz, R. (1988). Structural requirement for the rapid movement of charged molecules across membranes. *Biophys. J.* **54**, 25–33.
16. Mason, S.F. (1970). Color and the electronic state of organic molecules. In *The Chemistry of Synthetic Dyes.* (Venkataraman K., ed.) Academic Press, New York, USA.
17. Cogdell, R.J. & Frank, H.A. (1987). How carotenoids function in photosynthetic bacteria. *Biochim. Biophys. Acta.* **895**, 63–79.
18. Miki, W. (1991). Biological functions and activities of animal carotenoids. *Pure Appl. Chem.* **63**, 141–146.
19. Palozza, P. & Krinsky, N.I. (1992). Astaxanthin and canthaxanthin are potent antioxidants in a membrane model. *Arch. Biochem. Biophys.* **297**, 291–295.
20. Rich, M.R., De Strulle, R., Ferraro, G. & Brody, S.S. (1992). Dihydroxycarotenoid liposomes inhibit phototoxicity in *Paramecium caudatum.* *Photochem. Photobiol.* **56**, 413–416.
21. Jorgensen, K. & Skibsted, L.H. (1993). Carotenoid scavenging of radicals. Effect of carotenoid structure and oxygen partial pressure on antioxidative activity. *Z. Lebensm UntersForsch.* **196**, 423–429.
22. Cooper, R.D.G., Davis, J.B., Leftwick, A.P., Price, C. & Weedon, B.C.L. (1975). Carotenoids and related compounds. Part XXXII. Synthesis of astaxanthin, phoenicoxanthin, hydroxyechinenone, and the corresponding diosphenols. *J. Chem. Soc. Perkin I* 2195–2204.
23. Schaffer, P., Ahammer, H., Müller, W., Koidl, B. & Windisch, H. (1994). Di-4-ANEPPS causes photodynamic damage to isolated cardiomyocytes. *Pflügers Arch.* **426**, 548–551.
24. Cooney, R.V., Kappock, T.J.I., Pung, A. & Bertram, J.S. (1993). Solubilization, cellular uptake, and activity of β-carotene and other carotenoids as inhibitors of neoplastic transformation in cultured cells. *Methods Enzymol.* **214**, 55–68.
25. Tsien, R.Y. & Bacskai, B.J. (1995). Video-rate confocal microscopy. In *Handbook of Biological Confocal Microscopy.* (Pawley J.B., ed.), pp. 459–478, Plenum Press, New York, USA.
26. Weber, G. & Teale, F.W.K. (1957). Determination of the absolute quantum yield of fluorescent solutions. *Faraday Soc. Trans.* **53**, 646–655.
27. Mujumdar, R.B., Ernst, L.A., Mujumdar, S.R., Lewis, C.J. & Waggoner, A.S. (1993). Cyanine dye labeling reagents: sulfoindocyanine succinimidyl esters. *Bioconj. Chem.* **4**, 105–111.
28. Sens, R. & Drexhage, K.H. (1981). Fluorescence quantum yield of oxazine and carbazine laser dyes. *J. Luminescence.* **24/25**, 709–712.
29. Henderson, S.A., Spencer, M., Sen, A., Kumar, C., Siddiqui, M.A.Q. & Chien, K.R. (1989). Structure, organization, and expression of the rat cardiac myosin light chain-2 gene. *J. Biol. Chem.* **264**, 18142–18146.